



**Acoustics'08
Paris**
June 29-July 4, 2008

www.acoustics08-paris.org

Separated flow behavior in an in-vitro rigid model of the laryngeal channel

Denisse Sciamarella^a, Elisa Chisari^b, Guillermo Artana^b, Lucie Bailly^c and Xavier Pelorson^c

^aCNRS, Bâtiment 508, Université Paris-Sud, 91403 Orsay, France

^bLFD, Facultad de Ingenieria, Universidad de Buenos Aires, Av. Paseo Colon 850, C1063ACV Buenos Aires, Argentina

^cDépartement Parole & Cognition, GIPSA-lab, 46, avenue Félix Viallet, 38031 Grenoble Cedex, France
denisse@limsi.fr

Flow through an in-vitro rigid model of the laryngeal channel is measured using pressure sensors, and visualized using the Schlieren technique for different geometrical configurations. A quasi-impulsive upstream flow condition is used to simulate the jet emerging from the glottis at phonation onset. The separated flow behaviour in the presence of a ventricular constriction ("false vocal folds") is examined. Direct numerical simulations are proposed to assess the aerodynamic effects of the ventricular bands on the dynamics of the flow patterns involved.

1 Introduction

The ventricular bands, also commonly called "false vocal folds", are two mucous structures of the supraglottis, located superior to the laryngeal ventricle. Although their involvement during ordinary speech is usually not observed, many studies report their vibration during pathological and certain throat singing productions (*kargyraa*, *Sardinian "A Tenore"*) [1-3]. The exact physical origin of this behavior and its acoustical consequences is still under question.

In this research, we investigate the possible influence of supra-laryngeal structures on the glottal flow on the basis of in-vitro experiments. Pressure measurements on a mechanical replica of the larynx are first presented. These experiments are useful to test and to quantify the accuracy of theoretical models of the glottal flow developed to describe steady flowrate regimes of the jets.

Schlieren visualizations together with direct numerical simulation for the flow in the laryngeal channel allow gaining access, in addition, to the details of flow patterns formed in time-varying flow rate conditions. With these tools we have particularly studied the impulsive flow created when the flow starts to develop in a medium which is initially at rest.

2 In vitro replica

The experimental set-up is depicted on figure 1*.

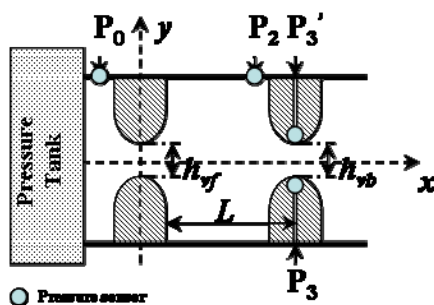


Figure 1 : Mechanical replica of the larynx including the false vocal folds

The set-up consists of a metallic replica of the human larynx. The laryngeal replica includes first a rigid 25 mm-thick vocal-folds replica having a rounded shape (radius of curvature of 6 mm). The vocal-folds replica is coupled to a rigid 25 mm-thick ventricular-bands replica also having a rounded shape (radius of curvature of 5 mm). The coupling between the vocal folds and the bands defines a ventricle

having a circular cross-section of a constant diameter ($h_{\text{ventricle}} = 26 \text{ mm}$). The glottal aperture h_{vf} as well as the ventricular aperture h_{vb} can be controlled parametrically with an accuracy of $\pm 0.05 \text{ mm}$.

A pressure reservoir supplies the set-up. The pressures respectively upstream, P_0 , within the separated region, P_2 , and within the ventricular-bands replica, P_3 , are measured using Kulite (XCS-0.93-0.35-Bar-G) or Endevco (8507C) pressure sensors supplied by a Labor-Netzgerat power supply (EA-3005S).

The sensor measuring P_2 is set 3 mm upstream of the ventricular-bands replica. P_3 is measured at the minimum constriction position within the ventricular-bands replica. An additional pressure sensor P_3' was also added to check for an asymmetry of the flow.

All pressure sensors are calibrated against an electronic manometer (Aschcroft XLdp) with typical accuracy of $\pm 5 \text{ Pa}$. Electrical signals are post-processed using a preamplifier/conditioning board (National Instruments SXCI-1121) connected to a PC through a National Instruments BNC-2080 Card and a National Instruments PCI-MIO-16XE acquisition card.

An example of results is presented in Figure 2. In this example $h_{\text{vb}}/h_{\text{vf}}$ is parametrically varied by changing the ventricular fold aperture h_{vb} while the alimentation pressure P_0 is maintained constant at 500 Pa.

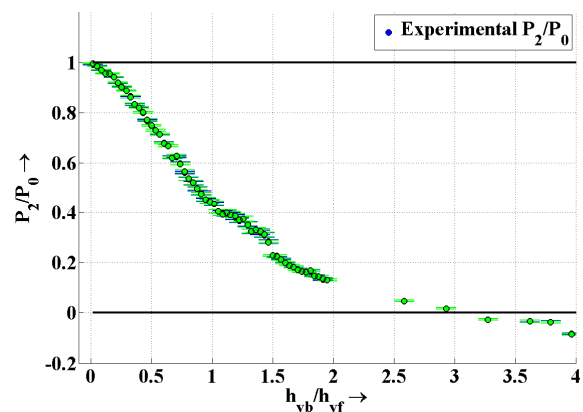


Figure 2: Normalized pressure recovery P_2/P_0 measured as a function of $h_{\text{vb}}/h_{\text{vf}}$.

As shown on Figure 2, the pressure P_2 decreases with $h_{\text{vb}}/h_{\text{vf}}$. More precisely, for $h_{\text{vb}}/h_{\text{vf}}$ in the range between ~ 0 up to ~ 3 , a significant pressure recovery is measured, reaching P_0 value for very small values of $h_{\text{vb}}/h_{\text{vf}}$. As a consequence, in this example, the pressure drop at the vocal folds decreases down to zero when $h_{\text{vb}}/h_{\text{vf}}$ tends towards 0, and in general, for higher values of $h_{\text{vb}}/h_{\text{vf}}$, the influence of the ventricular bands becomes progressively negligible.

Unsteady flow measurements can be performed on the same replica by opening a manual valve upstream of the

reservoir. A typical example of measurement is presented on figure 3 for two different ratio $h_{vb}/h_{vf} = 1$ and $h_{vb}/h_{vf} = 2$.

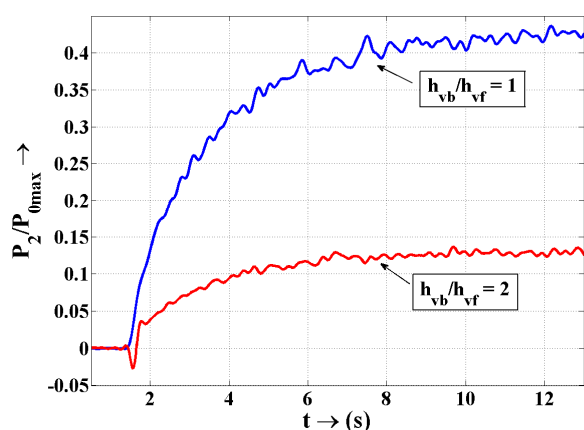


Figure 3 : Pressure recovery P_2/P_{0max} measured for unsteady flow measurements and for two different ratios h_{vb}/h_{vf} .

The example shown on Figure 3 enhances again the influence of h_{vb}/h_{vf} , and thus of the ventricular aperture, on the pressure recovery. It is also interesting to note the difference between the transients manually imposed in these experiments for the two different configurations. In the case of $h_{vb}/h_{vf} = 2$ a negative pressure P_2 is initially measured, this effect signals the importance of undertaking a careful analysis of the initial transient.

3 Schlieren visualizations

Our experimental set-up to analyse impulsive flows can be divided into two main parts. One of them is the Schlieren system (Figure 4), an optical system that allows us to observe index of refraction gradients in a transparent fluid. Changes of fluid density are the usual source of variations in the refraction index. The second part of the set-up consists of a pneumatic circuit that feeds a replica of the larynx (Figure 5).

The Schlieren system [4-6] built in our laboratory is a typical symmetrical Z-type system with two 0.50m diameter spherical mirrors with focal lengths of 3.0m. A rapid CMOS camera served as acquisition device for the Schlieren images, allowing recording frequencies of 50, 100 or 200 frames per second. Each time the frequency doubled, the spatial resolution of the image halved in the vertical direction. Both the illumination source and the knife-edges were placed at the mirror's focal distance.

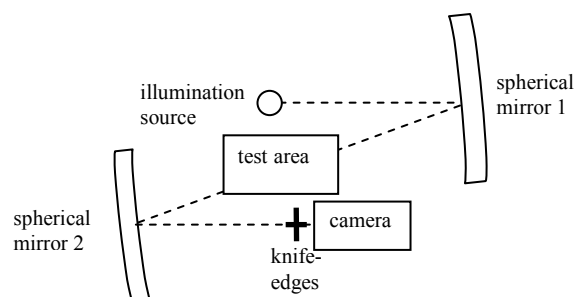


Fig.4 Diagram of the Z-type Schlieren system.

A pair of mutually perpendicular knife-edges placed in the focus of the second mirror helped to improve the contrast in the Schlieren images (otherwise we would observe images of Shadowgraph technique). Helium gas was introduced in the flow as a tracer through a lateral orifice immediately upstream the folds. A He compressed tank was used to feed the system with this gas. A pressure regulation immediately downstream the tank enabled us to control the mass flowrate of this gas, that always resulted quite reduced compared to the air mass flowing between the folds. As a consequence of the operation of the device with a small amount of tracer introduced in the flow the system enabled a very good contrast in the transients but not in the fully developed steady regimes.

The air pneumatic circuit mainly consisted of an approximately 400 dm³ recipient fed by a compressed air tank. The amplified signal from a calibrated differential pressure sensor was transmitted to a computer, which allowed us to monitor the pressure build-up inside the recipient when it is filled with dry air. Once the desired pressure was attained, the tank was isolated from the circuit by means of a two way valve. A system of hoses connected the recipient in series with a solenoid two way valve, a flow-meter and finally to the lower extreme of an 80 cm length and a 2.5 cm (inner) diameter aluminium tube. The response time of the solenoid valve (normally closed) at the opening operation is close to 5 msec.

The larynx replica was mounted on the tube's superior extreme, where pressure was equal to the atmospheric pressure. Thus, when the solenoid valve was energised, air flowed along the ducts from the recipient to the replica, passing through the vocal folds. The flow rate, which was conserved along the circuit, was measured in steady regime by the flow-meter. This value was chosen to be representative of a suitable airflow velocity between the vocal folds, and therefore set to 15 m/s, in accordance with typical values for the human larynx. Additionally, a replica representing the ventricular bands could be placed on top of the vocal folds and the parameters that can be varied in this geometry are the distance between the vocal folds (1 or 2mm), the separation between the ventricular bands (2, 4 or 6 mm) and the distance between the vocal folds and the ventricular bands (10, 20 or 30 mm).

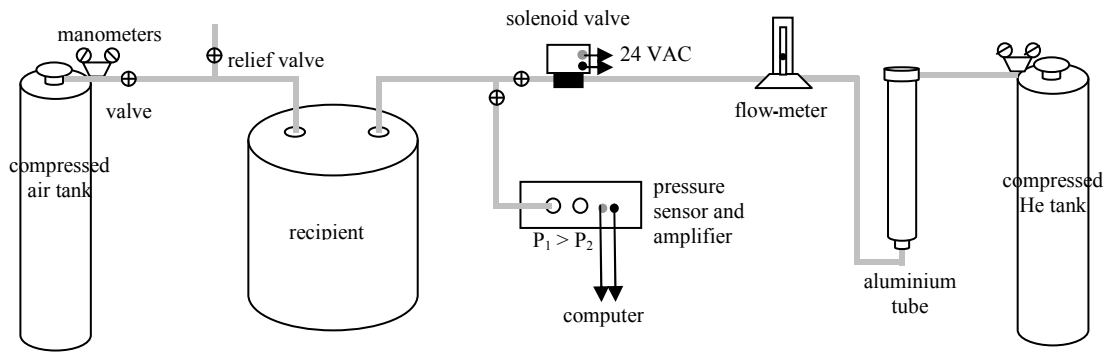


Fig.5 Diagram of the pneumatic circuit.

4 Numerical simulations

A multigrid finite-difference CFD method is proposed to simulate the airflow in the laryngeal channel. The advantage of multigrid methods is that the problem is not considered on a single mesh but on a set of successively refined meshes in order to help solve the finer scales. We use a fixed Cartesian grid that guarantees that the discretization scheme is not degraded by non orthogonal frames. The equations are integrated with a time marching algorithm based on a prediction projection method. The spatial discretization uses a staggered grid. The immersed boundaries are taken into account through a phase function equal to 0 or 1 for fluid or structure cells respectively.

The computational domain we consider is a rectangle of unit height and adjustable length, with $N_x \times N_z$ rectangular cells through which the boundaries can move freely. The Reynolds number is built on the channel's maximum height and the incoming velocity (Figure 6). The computations are performed on grids with $N_x=512$ or 1024 and $N_z=128$ or 256 . The time step is set to 10^{-4} or 10^{-5} . The narrower the constriction formed by the replica of the vocal folds, the higher the spatial resolution that is needed. For the lower spatial resolution, the coarse mesh is refined around the axis and next to the boundaries.

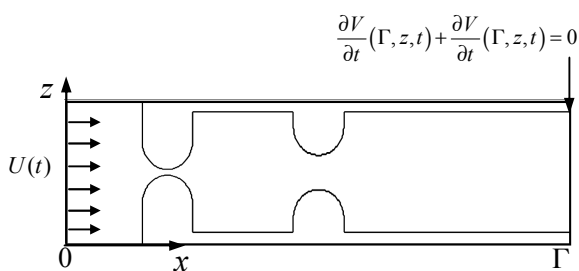


Fig.6 Laryngeal channel geometry and boundary conditions for the direct numerical simulations.

The design of the flow boundaries we have chosen corresponds to the geometry of the channel and replica used in the Schlieren experiment (figure 3). This includes configurations with either the vocal folds alone, or with both vocal folds and ventricular bands. Both the computational domain and the in vitro channel become slightly narrower in the transglottal region.

The incoming velocity has a square spatial profile in the transversal direction. Its value can be set either constant or time-dependent. We have performed numerical simulations with both a step flow and an initial linear ramp in order to match the response time of the solenoid valve. Velocities are set to zero in the structure cells. The inlet flow enters a channel where the fluid is initially still. On the solid walls we impose the classical no-slip and no-injection condition. At the downstream boundary, we impose the so-called advective-type boundary condition, the most natural boundary condition for a ‘transparent’ artificial boundary. This condition reduces to a homogeneous Neuman condition if the flow reaches a steady state. No symmetry condition is forced along the axis, to capture possible flow asymmetries. Further details on the numerical method are available in [7].

5 Results for impulsive flows

The initial transient can be significantly sensitive to the temporal dependence of the inlet velocity, especially for a highly constricted glottis (i.e. for a vocal fold separation of 1 mm). A step inflow condition, which is unrealistic since it would correspond to a valve with zero response time, will produce a non symmetrical and highly unstable jet, with a behaviour that resembles that of a jet immersed in a much more viscous media. This is not the case however if the glottal aperture is larger (i.e. for 2 mm). Let us recall that 5 msec is the time lag required for the solenoidal valve to open. After this transient, the value of the flow rate is kept constant in time, both in numerical and physical experiments. The maximum value of the flow rate is established in correspondance with the value measured with the flowmeter of the experimental set up at very large times, a value which is used to choose the Reynolds number for the numerical experience.

Three stages can be recognised in the evolution of the flow patterns observed in both, numerical simulations and experimental visualizations:

First stage: Jet formation

Numerical simulations show a plane jet that emerges from the vocal folds with a dipolar vortex front (symmetrical opposite-sign vortices forming a mushroom-like cap), which is typical of a pulsed injection of fluid (figure 7).

This mushroom structure is easy to identify in the Schlieren images. The head of the jet progresses along the duct with a convection speed which amounts to about 9 m/s for $Re=900$ and a 1 mm aperture for the vocal folds. This value is not significantly altered by the presence of the ventricular bands (figure 8). Along the boundary layers of opposite vorticity that delimit the evolving jet, it is possible to observe in the numerical experiments after a certain time, the subsequent formation of a series of smaller mushroom caps which were not present when the jet was formed.

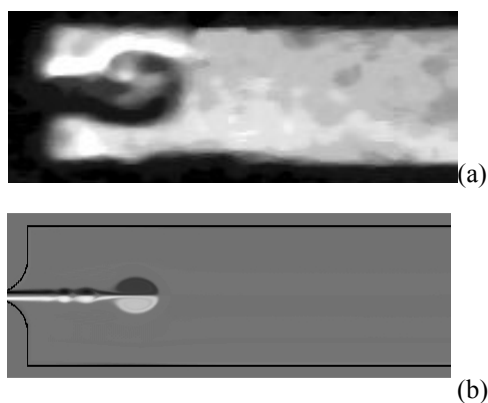


Fig.7 Jets emerging from the vocal folds at the initial stages of the flow onset with $Re=900$ without ventricular bands: (a) Schlieren Images, (b) Vorticity in numerical simulation

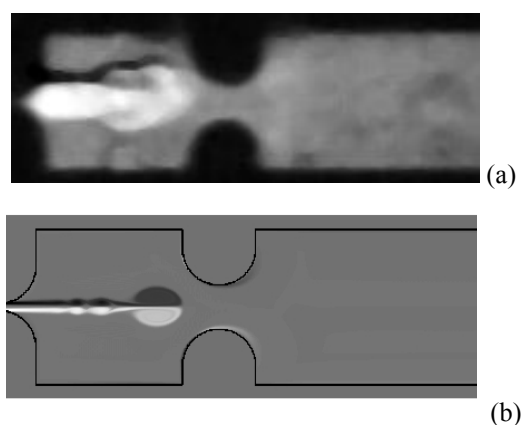


Fig.8 Jets emerging from the vocal folds at the initial stages of the flow onset with $Re=900$ with ventricular bands ($L=25\text{mm}$, $h_{vb}=6\text{mm}$): (a) Schlieren Images (b) Vorticity in numerical simulation

When the ventricular bands are present, a second jet is born at the exit of the ventricular bands (figure 9). This second jet is born simultaneously with the first jet if both structures (folds and bands) are equally constricted. If aperture at the bands is wider than the glottal aperture, there is a delay in the birth of the second jet which is proportional to the ratio between the band and fold apertures. The jet emerges from the ventricular bands at a speed which depends on the ventricular aperture: the less constricted the bands are, the slower the final jet progresses. The size of the jet past the ventricular bands (which is also determinant of the size of the mushroom-like cap of the final supralaryngeal jet) is also proportional to the ventricular aperture.

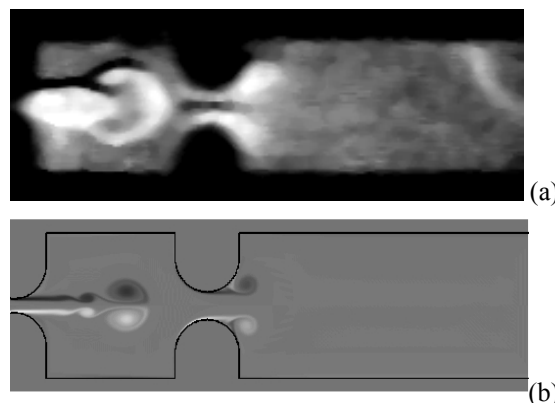


Fig.9 Jet emerging from the ventricular bands with $Re=900$ for a glottal opening of 2 mm and a band opening of 4 mm. $h_{vb}/h_{vf} = 2$. a) Schlieren Images b) Vorticity in Numerical Simulation

Second stage: Impinging of glottal jet on ventricular bands

The flow patterns in the ventricle after the instant in which the first jet (the glottal jet) impinges on the ventricular bands are quite complex in all the tested geometrical configurations. Small vortex dipoles are shed symmetrically in the upstream side of the walls of both ventricular bands. These vortex dipoles initiate a sinuous trajectory firstly away from the jet and then back towards the jet axis. The two relatively large vortex pairs of opposite sign which form in the ventricle after this phase (figure 10), tend to persist in all the numerical experiments performed with ventricular bands. This structure of symmetrical vortices of opposite sign in either side of the jet within the ventricle has also been found to be persistent in the Schlieren visualizations. The time needed for this structure to settle depends on $U(t)$ and h_{vb} .

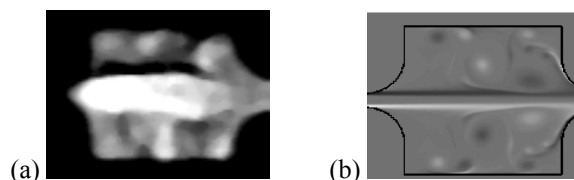


Fig.10 Persistent structure of symmetrical vortices of opposite sign within the ventricle for $Re=900$ in two different geometrical configurations: (a) Schlieren Images (b) Vorticity in numerical simulation

Third stage: loss of stability of the supralaryngeal jet

At larger times, a three dimensional flow pattern is observed for the flow past the ventricular bands (figure 11). At some distance from the ventricular bands a slug flow type is established that occupies the whole section. At the exit of the ventricular aperture, the jet is still visible, surrounded by vortical structures which are similar to the ones observed within the ventricle in the second stage of the flow. The 2D numerical simulation does not reproduce this 3D instability. Nevertheless, this late aerodynamic stage attained in the rigid replica of the larynx is actually never reached in phonation onset because of the fast flow modulation induced by vocal fold motion.

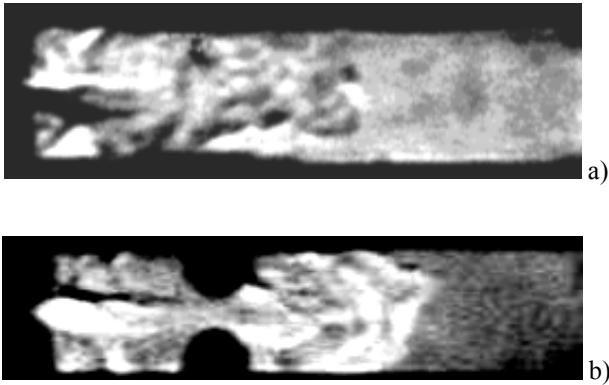


Figure 11 Loss of stability of the supralaryngeal jet
(a) Vocal fold (b) Ventricular bands

6 Discussion and perspectives

It is well known that the behaviour of flows in the early transients may differ significantly from well established steady regimes.

A study of pressure drops is carried out firstly, in order to quantify the influence of the ventricular bands for a progressive variation of their aperture under steady conditions.

Secondly, we perform numerical and physical experiments to better elucidate the characteristics of the impulsive accelerated jets produced at close vicinity of the (fixed and abducted) vocal folds and ventricular bands, in conditions which can be assimilated to those of phonation onset.

In these experiments, the ‘in vitro’ replica of the vocal folds and ventricular bands has rather simplistic features with a twofold purpose: facilitating the flow visualizations performed with the Schlieren technique and obtaining a planar flow which can be compared to 2D direct numerical simulations.

The trends observed in numerical simulations and Schlieren visualizations are in reasonable agreement when it comes to characterizing flow patterns in the initial stages of flow onset. This description allows highlighting some important aerodynamic phenomena that are likely to be present at the opening phase of the glottal cycle in the phonatory system. In particular, narrower ventricular apertures accelerate the formation of vortex structures which persist in the ventricular region. Such structures might impose their signature on flow behaviour past the ventricular bands. Further research is still necessary to elucidate these aspects.

Acknowledgments

This research has been partially supported by the project SticAmSud 07/06.

References

[1] Pinho, SMR, Pontes Pal, Gadelha MEC, Biasi N: Vestibular vocal fold behaviour during phonation in unilateral vocal fold paralysis. *Journal of Voice*, 13(1):36-42, 1999.

[2] Nasri S, Jasleen J, Gerratt BR, Sercarz JA, Wenokur R, Berke GS: Ventricular dysphonia: A case of the false vocal fold mucosal travelling wave. *American Journal of Otolaryngology*, 17(6):427-431, 1996.

[3] Fuks L, Hammarberg B, Sundberg J: A self-sustained vocal-ventricular phonation mode: Acoustical, aerodynamic and glottographic evidences. *KTH TMH-QPSR* 3:49-59, 1998.

[4] G. Settles, “Schlieren and Shadowgraph Techniques, Visualizing Phenomena in Transparent Media“ , *Springer-Verlag*, Berlin (2001).

[5] L. Vasil’ev, “Schlieren Methods”, *Israel Program for Scientific Translations Ltd.*, Keter Inc., New York (1971).

[6] W. Merzkirch, “Flow Visualization”, *Academic Press*, New York (1974).

[7] D. Sciamarella, P. Le Quéré, “Solving for unsteady airflow in a glottal model with immersed moving boundaries”, *European Journal of Mechanics B/Fluids* (2007), doi:10.1016/j.euromechflu.2007.06.004